Applied Catalysis B: Environmental 224 (2018) 469–478

Contents lists available at ScienceDirect

Applied Catalysis B: Environmental

journal homepage: www.elsevier.com/locate/apcatb

Research Paper

Low temperature reforming of biogas over K-, Mg- and Ce-promoted Ni/Al_2O_3 catalysts for the production of hydrogen rich syngas: Understanding the plasma-catalytic synergy

Y.X. Zeng[a], L. Wang[a], C.F. Wu[b,c], J.Q. Wang[b], B.X. Shen[b], X. Tu[a,*]

[a] Department of Electrical Engineering and Electronics, University of Liverpool, Liverpool L69 3GJ, UK
[b] School of Energy & Environmental Engineering, Hebei University of Technology, Tianjin, China
[c] School of Engineering, University of Hull, HU6 7RX, UK

ARTICLE INFO

Keywords:
Biogas reforming
Hydrogen production
Plasma-catalysis
CO_2 Utilization
Synergistic effect

ABSTRACT

Plasma-catalytic biogas reforming over Ni-X/Al_2O_3 catalyst (X = K, Mg and Ce) has been carried out in a coaxial dielectric barrier discharge (DBD) plasma reactor at 160 °C. Three different process modes: plasma-alone, catalysis-alone and plasma-catalysis have been investigated to get new insights into the synergistic effect resulted from the interaction of the plasma with the promoted Ni catalysts. Compared to the biogas reforming using either plasma-alone or catalysis-alone mode at the same temperature (160 °C), the combination of the plasma with the Ni-based catalysts exhibited a low temperature synergistic effect, as evidenced from the much higher reforming performance of the plasma-catalytic process compared to that of the sum of the individual processes (plasma-alone and catalysis-alone). The addition of promoters (K, Mg and Ce) into the Ni/Al_2O_3 catalyst enhanced the conversion of CH_4, the yield of H_2 and the energy efficiency of the plasma process. In this study, the behaviour of K, Mg and Ce promoters in the low temperature plasma-catalytic biogas reforming was clearly different from that in high temperature thermal catalytic process in terms of the conversion of CH_4 and carbon deposition, which could be ascribed to the temperature-dependent character of the promotors. In the plasma-catalytic biogas reforming, the Ni-K/Al_2O_3 catalyst showed the best performance, enhancing the conversion of both CO_2 and CH_4, the yield of H_2, CO and C_2–C_4 alkanes and the energy efficiency of the plasma process. The highest conversion of CO_2 (22.8%) and CH_4 (31.6%) was achieved by placing the K-promoted catalyst in the plasma reforming process. The Mg-promoted catalyst remarkably increased the H_2/CO molar ratio in the gas products (up to 2.2) due to the decreased CO_2 conversion. In addition, compared to the un-promoted Ni/Al_2O_3 catalyst, although the use of the promoted catalysts increased the carbon deposition on the surface of the spent catalysts by 22%–26%, the total amount of deposited carbon was still less than that reported in high temperature catalytic dry reforming processes. More than 80% of the increased carbonaceous species was in the form of reactive carbon species, which can be easily oxidized by CO_2 and O atoms and maintain the stability of the catalysts during the reforming reaction.

1. Introduction

Biogas is a renewable energy produced through anaerobic digestion of organic matter such as food scraps, manure, wastewater sludge, and crop residue. Biogas mainly consists of methane (50%–75%) and carbon dioxide (25%–50%). It also contains traces of hydrogen sulphide, water vapour, siloxanes, ammonia and halogenated compounds [1]. Biogas can be used for the generation of heat and electricity through combustion. However, the presence of CO_2 with a low heating value in the biogas lowers the overall efficiency for biogas utilization. An upgrading process is usually required to remove CO_2 in biogas to get biomethane. However, the separation of CO_2 is an energy intensive process. The reforming of biogas without prior CO_2 separation provides an attractive alternative for the more effective utilization of biogas. The produced syngas (a mixture of H_2 and CO) is an important chemical feedstock for the synthesis of a range of platform chemicals and synthetic fuels [2,3].

However, both CO_2 and CH_4 are highly stable, therefore high temperatures (> 700 °C) are usually required to achieve reasonable conversions of biogas and syngas yield due to the thermodynamic barrier of this reaction, resulted in high energy consumption. The rapid deactivation of reforming catalysts at high temperatures due to sintering and coke deposition remains a major challenge for the use of this process in

* Corresponding author.
E-mail addresses: xin.tu@liv.ac.uk, xin.tu@liverpool.ac.uk (X. Tu).

http://dx.doi.org/10.1016/j.apcatb.2017.10.017
Received 18 June 2017; Received in revised form 28 September 2017; Accepted 7 October 2017
Available online 08 October 2017

a commercial scale. Significant efforts have been devoted to the design and development of catalysts which can be used at a relatively low temperature with a high activity and coke resistance [4–7]. Recently, Debek et al. achieved a CH_4 conversion of 45% and a CO_2 conversion of 40% in thermal catalytic dry reforming of methane using a Ni-Mg-Al hydrotalcite-derived catalyst at a lower temperature (550 °C) [8]. Debek and his co-workers also found that the use of promoted hydrotalcite-derived catalysts could prevent the sintering of Ni species, but decreased the conversion of CH_4 and CO_2 compared to the catalysts without a promoter [9]. Further investigations are still required to improve the energy efficiency of the process through the decrease of reaction temperature and the development of novel highly active and stable reforming catalysts.

Non-thermal plasma (NTP) provides a promising alternative to thermal catalytic approach for the conversion of biogas into value-added chemicals and fuels (e.g., syngas) at low temperatures. NTP produces a range of highly reactive species and energetic electrons, subsequently activating and dissociating gas molecules even at ambient conditions, creating alternative reaction pathways, kinetically initiating and propagating thermodynamically unfavourable reactions at low temperatures. Non-thermal plasma chemical processes have the flexibility to be combined with renewable energy sources such as wind, tidal, hydraulic or solar power to reduce energy cost for localized or distributed energy storage. In the plasma conversion of greenhouse gas (e.g. CO_2 decomposition and dry reforming), a trade-off between the conversion of reactants and the energy efficiency has been often observed, remaining a challenge for the development of highly efficient plasma chemical processes [10]. The combination of the plasma with a catalyst has great potential to overcome this barrier and to generate a synergistic effect resulted from the interactions between the plasma and catalyst, which can enhance the reaction performance in terms of the conversion, the selectivity and yield of target products and the energy efficiency of the plasma process [11–16]. For instance, Tu et al. found that packing a commercial Ni/Al_2O_3 catalyst into the whole discharge region of a DBD reactor decreased the conversion of CH_4 and CO_2 compared to the plasma dry reforming reaction without packing a catalyst, which means that the coupling of the plasma with the catalyst did not generate a plasma-catalytic synergy. They suggested that the synergistic effect of the combination of plasma with a catalyst for hydrocarbon reforming depends on the balance between the change in discharge behaviour induced by the catalyst and the activity of the catalyst assisted by the plasma [17]. In their recent works, Tu and Whitehead reported a low temperature (~250 °C) plasma-catalytic synergy when placing a Ni/Al_2O_3 catalyst in the plasma dry reforming of methane using a partial packing method, which showed both the conversion of CH_4 and H_2 yield were almost doubled compared to the same reaction using plasma alone [15]. This significant synergistic effect of plasma-catalysis can be attributed to both strong plasma-catalyst interactions due to partial packing and resulted high activity of the catalyst at low temperatures [15]. More recently, we reported a significant enhancement of CH_4 yield in the plasma-catalytic hydrogenation of CO_2 over a Ni catalyst due to the formation of the plasma-catalytic synergy [18].

Compared with conventional thermal catalytic reactions, the hybrid plasma-catalytic process can be operated at low temperatures even room temperature without extra heating, with a very unique advantage of instant start-up and shut-down, which can significantly reduce the energy cost of the plasma process. In the past few years, increasing efforts have been devoted to the plasma-assisted reforming of CH_4 and CO_2 in the form of different sources (e.g., biogas or landfill gas) for the production of syngas at low temperatures, with or without a catalyst [10,13,19–24]. However, comparing against thermal catalytic biogas reforming, very few catalysts (mainly Ni based catalysts) have been developed and evaluated in the plasma-catalytic biogas reforming process [25–27]. The knowledge of selecting appropriate catalysts for highly efficient plasma dry reforming process is still very limited. The synergistic effect between the NTP and the catalyst is not yet fully understood.

Interestingly, Ni/Al_2O_3 catalyst has been extensively used for the conventional thermal catalytic biogas reforming process, while metal species such as K, Na, Ca, Mg, Y, La and Ce have been used as a modifier to enhance catalytic performance [5,9,28–37]. K, Mg and Ce promoters, for example, have been reported to significantly reduce coke deposition on the catalyst surfaces, resulted in an enhanced stability of the catalytic performance in catalytic reforming processes [28,29,31,35,37,38]. However, to the best of our knowledge, the properties and reaction performance of the promoted catalysts in the plasma-catalytic reforming process are largely unknown; while the effect of adding promoters to the catalysts on the low temperature plasma-catalytic biogas reforming has not been investigated. Moreover, the potential plasma-catalytic synergy is yet to be confirmed and investigated. Therefore, significant fundamental works are still essential to evaluate the catalysts promoted by different elements for the low temperature plasma biogas reforming process, and the catalytic performance is to be examined with and without using NTP.

In this work, a temperature controlled reactor has been developed for the reforming of biogas into syngas at low temperatures under different process modes: plasma-alone, catalysis-alone and plasma-catalysis, to get new insights into the synergistic effect resulted from the interaction between the plasma and the catalysts. The influence of K-, Mg- and Ce-promoted Ni/Al_2O_3 catalysts on the plasma-catalytic biogas reforming has been evaluated in terms of the conversion of the reactants, the yield of gas products, the H_2/CO molar ratio and the energy efficiency of the process. Different characterization techniques including X-ray diffraction (XRD), N_2 adsorption-desorption (BET), Temperature programmed reduction (H_2-TPR), Temperature programmed desorption (CO_2-TPD and NH_3-TPD) and Thermal gravimetric analysis (TGA) have been used to understand the physiochemical properties of the catalysts and their effects on the reforming process at low temperatures. The carbon deposition on the spent catalysts after the plasma-catalytic reforming process was also examined.

2. Experimental

2.1. Experimental setup

Fig. 1 shows a schematic diagram of the plasma-reforming system. The experiments were carried out in a coaxial packed-bed DBD reactor. A quartz tube with an outer diameter of 21 mm and a wall thickness of 2.5 mm was used as a dielectric layer. A stainless-steel mesh wrapped around the quartz tube served as a ground electrode, while a stainless-steel rod was placed in the axis of the quartz tube and acted as a high voltage electrode. The discharge length was 100 mm with a discharge gap of 1.5 mm. The DBD reactor was connected to a high voltage AC power supply with a maximum peak voltage of 10 kV. The voltage on an external capacitor (C_{ext} = 0.47 μF) connecting the ground electrode and ground was measured to determine the total charge (Q_{ext}) transferred in the plasma reaction, while the applied voltage was measured by a high voltage probe (Testec, HVP-15HF). Both signals were recorded by a digital oscilloscope (Tektronix MDO3014). The discharge power was determined by calculating the area of the Q-U Lissajous figure. A homemade power measurement system was used to monitor and control the discharge power in real time. In this work, the discharge power was fixed at 16 W.

A simulated biogas with a CH_4/CO_2 molar ratio of 1.5 (60 vol.% CH_4 and 40 vol.% CO_2, no dilution) was used as reactants and the total flow rate was fixed at 50 ml min^{-1}. The 8 wt.% Ni/Al_2O_3 and 8 wt.% Ni– 2 wt.% X/Al_2O_3 (X = K, Mg and Ce) catalysts were prepared by the wetness co-impregnation using nitrate salts (Alfa Aesar, ACS reagents) as the metal precursor. Catalyst support (granular Al_2O_3) was added to the solution of nitrate salt, and the resulting slurry mixture was continuously stirred for 1 h and impregnated for 3 h, then dried at 90 °C

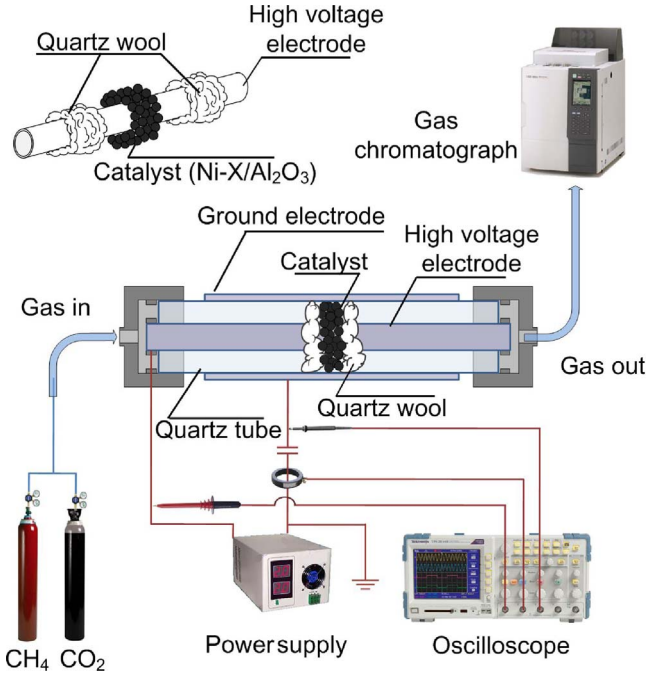

Fig. 1. Schematic diagram of experimental setup.

overnight, followed by calcination at 400 °C for 4 h. A total amount of 0.4 g Ni catalyst was packed into the reactor and sandwiched by quartz wool. Prior to the reforming reaction, the catalyst was reduced in an argon-hydrogen discharge at a discharge power of 16 W (50 ml min^{-1}, 20 vol.% H_2) for 30 min in the same DBD reactor. The catalysts, Ni/Al_2O_3, Ni-K/Al_2O_3, Ni-Mg/Al_2O_3 and Ni-Ce/Al_2O_3 are denoted as NiAl, NiKAl, NiMgAl and NiCeAl in the following sections, respectively.

The DBD reactor was placed in a tube furnace, which enabled the biogas reforming to be investigated at the same temperature under three different process modes: plasma-alone, catalysis-alone and plasma-catalysis. Under the plasma-alone mode, no catalyst was placed in the DBD reactor and the reaction was only driven by the plasma without extra heating. In thermal catalytic reaction (catalysis-alone mode), the catalyst was packed into the middle of the reactor and heated in the tube furnace without using the plasma. In the plasma-catalytic process, the catalyst was directly placed in the DBD reactor with interactions between the plasma and the catalyst. The temperature inside the reactor was 160 ± 5 °C for all three operating modes, measured by a fibre optical thermometer (Omega FOB102). However, only in the thermal-catalytic process, the reactor was heated by the tube furnace, while no extra heating was provided to the plasma process with or without a catalyst.

The gaseous products were analyzed by a two-channel gas chromatograph (Shimadzu GC-2014) equipped with a flame ionization detector (FID) and a thermal conductivity detector (TCD). Each measurement was repeated for three times after running the reaction for about 1 h when a steady state has been reached.

2.2. Catalyst characterization

N_2 adsorption–desorption analysis was performed at −196 °C to measure the pore size and specific surface area of the catalysts (Micrometrics ASAP 2020 instrument, USA). Prior to the measurement, the samples were outgassed at 350 °C for 3 h under vacuum to remove moisture and other adsorbed gases. The specific surface area of the samples was calculated using the Brunauer–Emmett–Teller (BET) method. XRD patterns of the catalyst samples were measured by an X–ray diffractometer (Rigaku D–Max 2400, Cu–K_α radiation, Japan) in the 2θ scanning range between 10° and 80°. The reducibility of the catalysts was determined by temperature–programmed reduction with hydrogen (H_2–TPR) using an automated chemisorption system (Quantac chrome ChemBET 3000, USA). Before each measurement, the sample was firstly treated at 400 °C for 1 h in a He flow at 20 ml min^{-1}. After cooled to 150 °C, the sample was saturated with H_2 for 30 min and then purged with a He flow at 150 °C for 1 h. The carbon deposition on the spent catalysts was determined by thermal gravimetric analysis (TGA) in an air atmosphere using a TA Instruments SDT-Q600 system. The spent catalyst was heated from 30 °C to 800 °C at a heating rate of 10 °C min^{-1} in an air flow of 30 ml min^{-1}. The NH_3-TPD and CO_2-TPD of the catalysts were measured using a Chemisorption analyzer (PCA-1200, Beijing Aode). Before each measurement, 50 mg catalyst sample was pre-treated at 200 °C for 1 h in a N_2 flow at 30 ml min^{-1}. The adsorption of NH_3 was carried out at 100 °C for 1 h in a NH_3 flow at 50 ml min^{-1}, then purged with a N_2 flow at 100 °C for 30 min. The adsorption of CO_2 was operated at 50 °C for 30 min in a CO_2 flow at 30 ml min^{-1}, followed by a N_2 purge for 30 min. The desorption of NH_3 or CO_2 was performed in a TGA equipment (SDTQ600). The catalyst sample was heated from 30 °C to 800 °C at a heating rate of 10 °C min^{-1}.

2.3. Definition of calculations

For the biogas reforming, the conversion (X) of CH_4 and CO_2 is defined as:

$$X_{CH_4}(\%) = \frac{CH_4 \text{ converted (mol)}}{CH_4 \text{ input (mol)}} \times 100 \quad (1)$$

$$X_{CO_2}(\%) = \frac{CO_2 \text{ converted (mol)}}{CO_2 \text{ input (mol)}} \times 100 \quad (2)$$

The selectivity (S) and yield (Y) of the main products are calculated as:

$$S_{CO}(\%) = \frac{CO \text{ produced (mol)}}{CO_2 \text{ converted (mol)} + CH_4 \text{ converted (mol)}} \times 100 \quad (3)$$

$$S_{H_2}(\%) = \frac{H_2 \text{ produced (mol)}}{2 \times CH_4 \text{ converted (mol)}} \times 100 \quad (4)$$

$$S_{C_xH_y}(\%) = \frac{x \times C_xH_y \text{ produced (mol)}}{CO_2 \text{ converted (mol)} + CH_4 \text{ converted (mol)}} \times 100 \quad (5)$$

$$Y_{CO}(\%) = \frac{CO \text{ produced (mol)}}{CO_2 \text{ input (mol)} + CH_4 \text{ input (mol)}} \times 100 \quad (6)$$

$$Y_{H_2}(\%) = \frac{H_2 \text{ produced (mol)}}{2 \times CH_4 \text{ input (mol)}} \times 100 \quad (7)$$

$$Y_{C_xH_y}(\%) = \frac{x \times C_xH_y \text{ produced (mol)}}{CO_2 \text{ input (mol)} + CH_4 \text{ input (mol)}} \times 100 \quad (8)$$

The H_2/CO molar ratio in the product is determined as:

$$\frac{H_2}{CO} = \frac{H_2 \text{ produced (mol)}}{CO \text{ produced (mol)}} \quad (9)$$

The total energy efficiency for the conversion of CH_4 and CO_2 (E) [13], fuel production efficiency (FPE) of biogas reforming [26], and synergy capacity (SC) of the plasma-catalysis [39] are calculated as follows:

$$E(\text{mmol kJ}^{-1}) = \frac{CH_4 \text{ converted (mol s}^{-1}) + CO_2 \text{ converted (mol s}^{-1})}{\text{Discharge power (W)}} \quad (10)$$

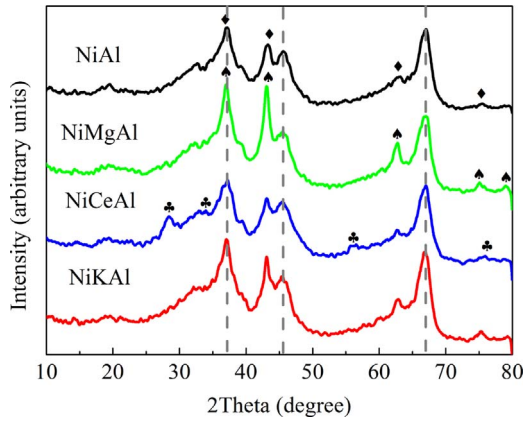

Fig. 2. XRD patterns of fresh catalysts. (♦ NiO, ♠ MgO, ♣ CeO_x, and dash line γ–Al_2O_3).

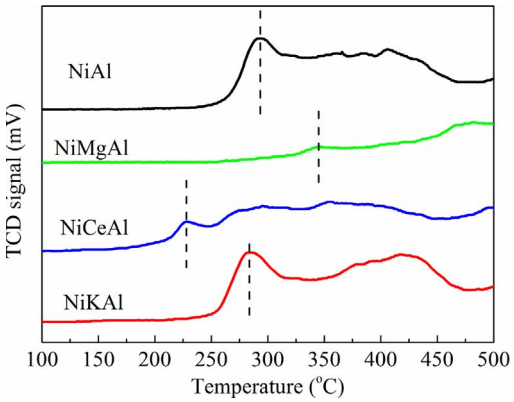

Fig. 3. H_2–TPR profiles of the fresh catalysts.

$$\text{FPE}\ (\%) = \frac{\text{LHV}_{CO}(\text{J mol}^{-1}) \times \text{CO produced(mol s}^{-1}) + \text{LHV}_{H_2}(\text{J mol}^{-1}) \times \text{H}_2\ \text{produced(mol s}^{-1})}{\text{LHV}_{CH_4}(\text{J mol}^{-1}) \times \text{CH}_4\ \text{input(mol s}^{-1}) + \text{discharge power(W)}} \times 100 \quad (11)$$

$$SC_{\zeta}(\%) = \frac{\zeta_{p+c} - \zeta_p - \zeta_c}{\zeta_p + \zeta_c} \times 100 \quad (12)$$

where LHV is the lower heating value of the corresponding combustible gas. Only H_2 and CO are considered in Eq. (11) in order to compare with other reported works. ζ can be conversion, selectivity, yield, or fuel production efficiency. The subscript p + c, p, and c represent the results obtained from plasma-catalysis, plasma-alone, and catalysis-alone, respectively.

3. Results and discussion

3.1. Catalyst characteristics

Fig. 2 shows the XRD patterns of the catalysts. Three diffraction peaks at 2θ = 37.6°, 45.9° and 67.0° corresponded to the formation of a cubic structure of alumina crystallite (JCPDS 10–425), while the diffraction peaks of NiO (JCPDS 1–75–197) were also identified for all the catalysts. However, only weak reflection of CeO_x (JCPDS 3–65–5923) crystallite was detected. Some of the MgO peaks were overlapped with those of NiO [40,41], thus the diffraction peaks of MgO (JCPDS 1–1235) crystallite were also weak. Note that the diffraction peaks of cubic K_2O (JCPDS 23–493) were not observed [42], which suggests that K species could be well dispersed on the catalyst surface or existed in amorphous form [43]. The crystallite size of the catalysts was estimated using Scherrer equation, as summarized in Table 1 [44]. The average size of NiO crystallite on the NiAl catalyst was 6 nm, and increased to 10 nm with the addition of Mg to the NiAl catalyst. Similar phenomenon of increased crystalline size on promoted catalysts has also been reported in thermal catalytic reforming [28,35]. Notably, a few promoters (e.g. adding La into Co/ZrO_2) have been reported to enhance the dispersion of active metal species on the surface of the catalyst. However, K, Mg and Ce promoters have been observed to agglomerate active metal species and resulted in larger particle sizes [31], which generally increases coke deposition on the catalyst surfaces [45–47]. However, in thermal catalytic processes, the K, Mg and Ce promoters preferentially bind to "coking sites" and suppress the formation of graphite, without significantly affecting the reforming performance [48].

Table 1
Physicochemical characteristics of fresh catalysts.

Catalyst	Specific surface area ($m^2\ g^{-1}$)	Total pore volume ($cm^3\ g^{-1}$)	Average crystallite size (nm)
NiAl	165	0.29	6
NiMgAl	160	0.25	10
NiCeAl	158	0.29	7
NiKAl	152	0.29	8

Table 1 shows the physicochemical properties of the catalysts. The BET specific surface area of the NiAl catalyst was 165 $m^2\ g^{-1}$, while the addition of the promoters to the NiAl catalyst slightly decreased the BET specific surface area of the catalysts (152–160 $m^2\ g^{-1}$). The BET area of the catalysts followed the order of NiAl > NiMgAl > NiCeAl > NiKAl.

The reducibility of supported metal catalysts is a critical factor affecting the catalytic activity. Fig. 3 shows the H_2–TPR result of the fresh catalysts. On the TPR profile of the NiAl catalyst, the first peak at 290 °C corresponded to the reduction of bulk NiO, while the overlapping peak at 410 °C can be assigned to the reduction of less active NiO. The less active NiO had a higher reduction temperature due to its stronger interaction with the support of the catalyst [49,50]. The addition of K, Mg and Ce promoters showed different effects on the reducibility of the Ni-based catalysts. The TPR profile of the NiKAl catalyst was similar to that of the NiAl catalyst except that the reduction temperature of bulk NiO decreased to 260 °C. For the NiMgAl catalyst, the reduction temperature of bulk NiO increased to 340 °C. The intensity of the peak associated to the reduction of NiO was diminished, which might be attributed to the intensified interaction between NiO and Al_2O_3 promoted by the presence of Mg species [51,52]. The reduction of bulk NiO on the NiCeAl catalyst occurred at 230 °C, which was clearly the lowest reduction temperature among the catalysts. However, such reduction proceeded over a wide temperature range (230 °C–450 °C), while the portion of the bulk NiO on the catalyst was lower than that of the NiAl and NiKAl catalysts, which suggests that the NiCeAl catalyst might have a weak catalytic activity compared to the NiAl and NiKAl catalysts.

The adsorption of CO_2 on the surface of the catalysts plays a critical role in the catalytic reforming reaction [53,54]. The CO_2-TPD profile of the NiAl catalyst showed a strong peak located at 500 °C (Fig. 4), which can be associated to the desorption of CO_2 from strong basic sites on the catalyst surface. By contrast, negligible peaks were found below 400 °C, which could be related to CO_2 desorption from weak or medium basic sites on the catalyst surface. The addition of Mg promoter significantly decreased the CO_2 desorption over 400 °C, indicating the quantity of strong basic sites on the catalyst has been decreased by the Mg addition. Compared to the NiAl catalyst, adding Ce promoter decreased the desorption temperature from 500 °C to 480 °C, which suggests that the desorption of CO_2 from strong basic sites was slightly weakened.

Fig. 4(b) shows the NH_3-TPD profiles of the catalysts. On the NH_3-TPD profile of the NiAl catalyst, three peaks located at 170 °C, 310 °C and 520 °C can be observed. The peak below 400 °C corresponded to the

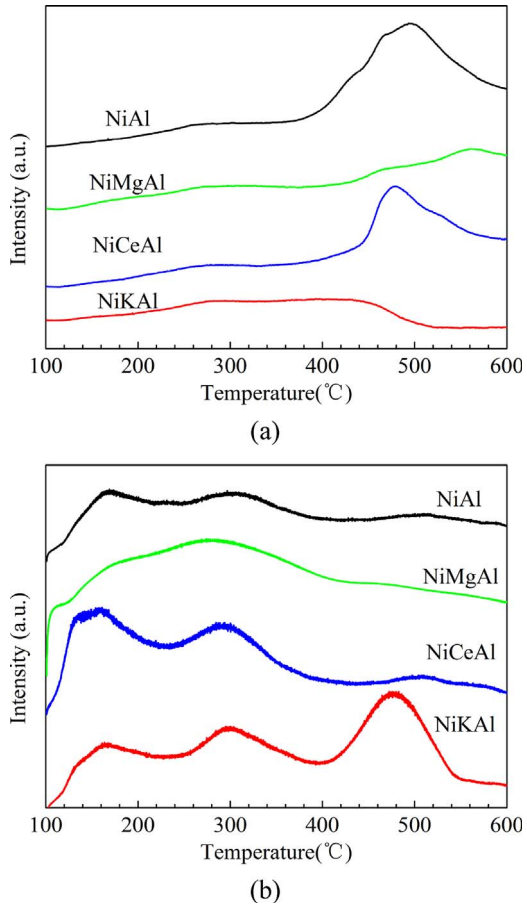

Fig. 4. TPD profiles of fresh catalysts. (a) CO_2-TPD, (b) NH_3-TPD.

desorption of NH_3 from weak and medium acid sites, while the desorption peaks over 400 °C could be associated to NH_3 desorption from strong acid sites [55–58]. It is noted that most of NH_3 desorption happened below 400 °C. For comparison, the addition of Mg promoter increased the NH_3 desorption from medium acid sites as the desorption temperature of NH_3 on medium acid sites decreased from 300 °C to 280 °C. The introduction of Ce species enhanced the NH_3 desorption from weak and medium acid sites. Interestingly, the addition of K promoter significantly increased NH_3 desorption from strong acid sites. All the results suggest that the presence of promoters improved the acidity of the catalysts, in particular for the NiKAl catalyst.

3.2. Biogas reforming under different operating modes

Fig. 5 shows the conversion of CH_4 and CO_2 in the biogas reforming process at the same temperature of 160 °C under three different operating modes: plasma-alone, catalysis-alone and plasma-catalysis. A plasma-catalytic synergy can be clearly identified when placing the NiKAl catalyst in the DBD reactor. At such a low temperature, the reforming reaction can only be initiated in the presence of a plasma, regardless of the use of a catalyst. In the catalysis-alone mode without plasma, the conversion of CH_4 and CO_2 was negligible at 160 °C due to the thermodynamic limitation of this reaction at low temperatures. By contrast, the conversion of CH_4 and CO_2 in the plasma biogas reforming at the same temperature of 160 °C was 25.1% and 18.2%, respectively. These findings suggest that non-thermal plasmas can enable thermodynamically unfavourable biogas reforming reaction to occur at low temperatures.

Fig. 6(a) shows the effect of different catalysts on the conversion of CH_4 and CO_2. Compared to the plasma biogas reforming over the NiAl catalyst, the coupling of DBD with the promoted catalysts enhanced the

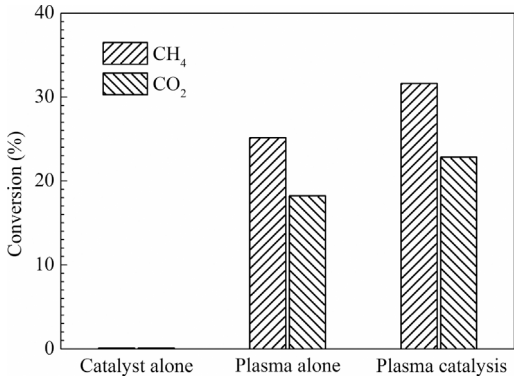

Fig. 5. Conversions of CH_4 and CO_2 under different process modes using the NiKAl catalyst.

conversion of CH_4, which was consistent with the enhanced acidity of the promoted catalysts, suggesting the acidic sites on the surface of these catalysts contributed to the activation of CH_4. However, only the K- and Ce-promoted Ni catalysts showed enhanced conversion of CO_2, while placing the Mg-promoted Ni catalyst in the plasma decreased the CO_2 conversion, which could be ascribed to the decreased basic sites and weak CO_2 affinity on the surface of the NiMgAl catalyst, as shown in Fig. 4(a). In the plasma-catalytic biogas reforming, considering the overall conversion of both gases, the best conversion was achieved by using the NiKAl catalyst, closely followed by the NiCeAl catalyst.

Interestingly, previous works on high temperature catalytic dry reforming of methane demonstrated that the use of K- and Ce-promoted Ni/Al_2O_3 catalysts decreased the conversion of CH_4 and CO_2 compared to Ni/Al_2O_3 catalyst under the same conditions [28,29]. By contrast, Mg promoted catalyst showed higher conversion of CO_2 compared to un-promoted catalysts [33,35,37]. For instance, Nandini et al. carried out thermal catalytic biogas reforming over Ni-based catalysts at 800 °C, with a feed gas ratio CH_4: CO_2: N_2 of 1: 1: 0.9. Compared to the Ni/Al_2O_3 catalyst, the addition of 0.5 wt.% K into the Ni/Al_2O_3 catalyst decreased the conversion of CH_4 from 84.7% to 70.2%, and the CO_2 conversion from 81.4% to 72.1%, respectively [28]. Alipour et al. evaluated the performance of thermal catalytic dry reforming at 650 °C using 5 wt.% Ni/Al_2O_3 catalysts with and without a promoter. They reported that the conversion of CO_2 was enhanced from 66% to 77% with the addition of 3 wt.% Mg to the Ni catalyst [35]. By contrast, Wang et al. investigated thermal catalytic DRM over a $NiO\text{-}CeO_2\text{-}Al_2O_3$ (Ni-Ce-Al) catalyst prepared by an improved one-pot evaporation-induced self-assembly (EISA) method [34,59]. They found that increasing the Ce/Al molar ratio of the Ni-Ce-Al catalyst from 0 to 1:50 significantly increased the conversion of CH_4 and CO_2 from 60% to 80% and from 59% to 73%, respectively [59]. These results show that the effects of K, Mg and Ce promotors on biogas reforming are different for low temperature plasma reactions and high temperature thermal catalytic reactions. Such difference is more likely related to the temperature-dependent character of the promoters in reforming reactions [35]. For instance, Alipour et al. reported that compared with a NiAl catalyst, the addition of Ca promoter increased the CO_2 conversion at 550 °C in thermal catalytic biogas reforming, but the conversion of CO_2 was decreased at 700 °C [35]. In addition, the TPD analysis in this study showed that the promoted catalysts had different adsorption and desorption behavior under low and high temperatures (Fig. 4), leading to different catalytic effects in low temperature plasma reactions and high temperature catalytic processes.

Fig. 6(b) shows the selectivity of H_2 and CO in the plasma biogas reforming with or without a catalyst. Compared to the plasma-alone mode, the presence of the catalysts in the DBD reactor clearly decreased the selectivity of CO, while only the NiKAl catalyst effectively improved the H_2 selectivity with the highest value of 43.3% in the plasma-catalytic biogas reforming. The combination of the DBD with the NiMgAl

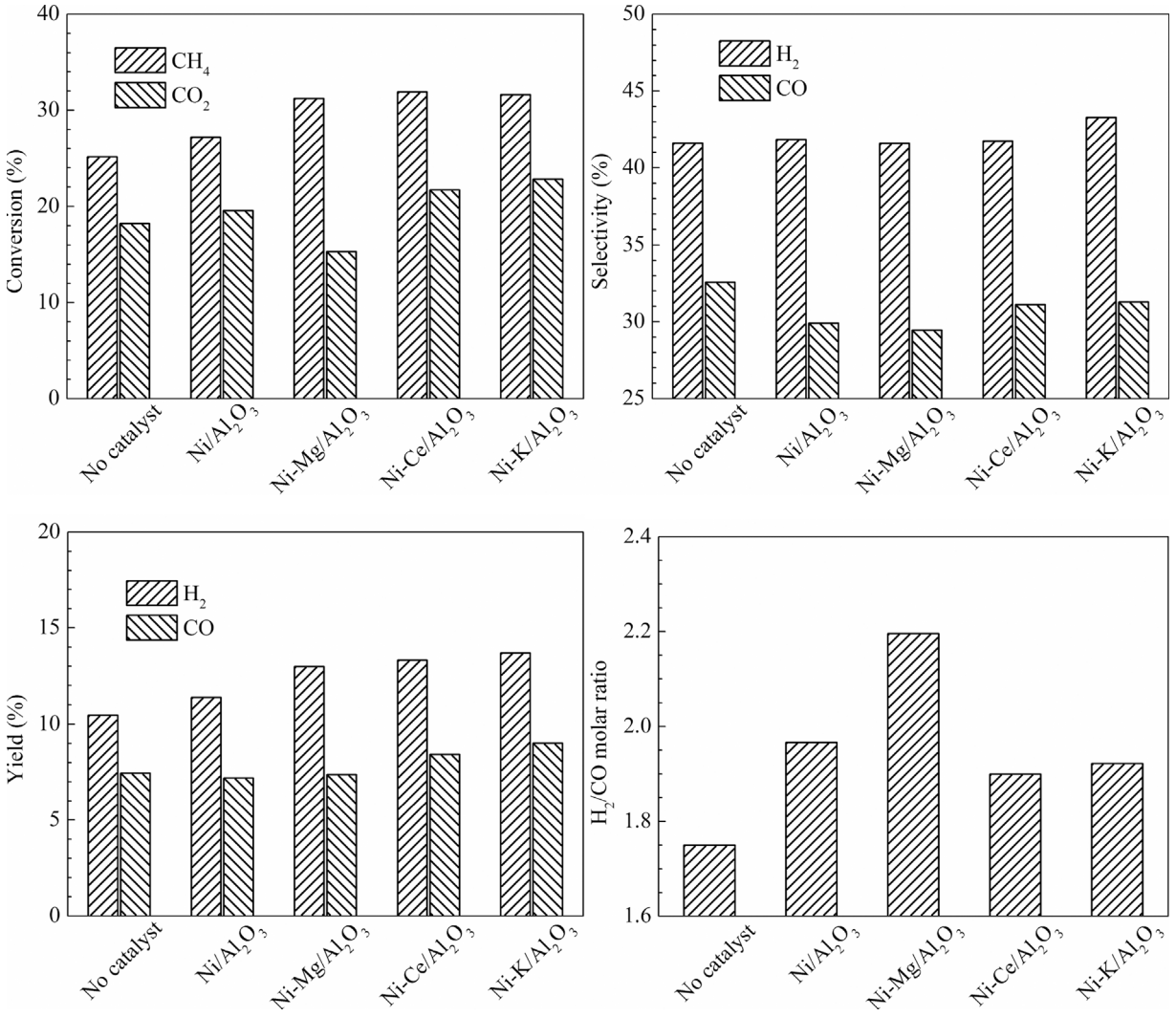

Fig. 6. Effect of different catalysts on (a) Conversion of CH_4 and CO_2, (b) Selectivity and (c) Yields of H_2 and CO, and (d) H_2/CO molar ratio.

catalyst exhibited the lowest CO selectivity (29.4%) as CO production is closely related to the conversion of CO_2. Compared to the plasma biogas reforming without a catalyst, placing the catalysts in the DBD reactor enhanced the yield of H_2 (Fig. 6(c)), which was consistent with the effect of these catalysts on the conversion of CH_4 (Fig. 6(a)). However, the CO yield was only improved over the NiKAl and NiCeAl catalysts as the coupling of the plasma with the NiMgAl catalyst suppressed the conversion of CO_2.

Fig. 6(d) shows that the presence of the catalysts in the plasma enhanced the H_2/CO molar ratio, which can be attributed to the different effects of the catalysts on the conversion of CH_4 and CO_2. The highest H_2/CO ratio of 2.2 was achieved when using the NiMgAl catalyst in the plasma reforming as this catalyst had the lowest CO_2 conversion even compared to the plasma reaction without a catalyst. Interestingly, the H_2/CO molar ratio obtained over different catalysts followed the order: NiCeAl < NiKAl < NiAl < NiMgAl, exactly the reversed order as the reducibility of these catalysts. This is plausible since the production of CO is strongly dependent on the conversion of CO_2, while the CO_2 conversion is affected by the reducibility and basicity of the catalysts [36].

Saturated hydrocarbons including ethane, propane and butane, together with unsaturated ethylene and acetylene were detected in the plasma biogas reforming, as shown in Fig. 7. The amounts of alkanes in the gaseous products were two orders of magnitude higher than that of unsaturated hydrocarbons. Therefore, only the selectivity and yield of alkanes are presented in this paper. The highest selectivity towards ethane and propane was achieved in the plasma biogas reforming over the NiMgAl catalyst, while the NiKAl catalyst showed the lowest selectivity to ethane and propane. All the catalysts had a similar selectivity of butane. Note that butane was generated only in the plasma-catalytic reforming reaction. In addition, the use of these catalysts improved the yield of C_2–C_4 alkanes. Compared to the plasma-alone mode, the combination of the DBD with the NiKAl catalyst enhanced the yield of ethane and propane by 16.5% and 25.5%, respectively, which can be ascribed to the significant enhancement of CH_4 conversion in the plasma-catalytic coupling mode.

Fig. 8 shows the influence of the catalysts on the energy efficiency of the plasma biogas reforming process. Clearly, compared to the plasma-alone reaction, the plasma-catalytic coupling enhanced the total energy efficiency and fuel production efficiency due to the generation of the plasma-catalytic synergy at low temperatures. In the plasma-catalytic biogas reforming, the use of K-, Mg- and Ce-promoted catalysts showed higher energy efficiency compared to the plasma reaction over the unpromoted NiAl catalyst. The highest energy efficiency (0.67 mmol kJ^{-1}) and fuel production efficiency (14.4%) were achieved when placing the NiKAl catalyst in the plasma reforming process. Table 2 presents a summary of the energy efficiency of plasma biogas reforming using different DBD systems under similar conditions.

In this work, synergistic capacity is introduced to quantify the reaction performance of the plasma-catalytic biogas reforming,

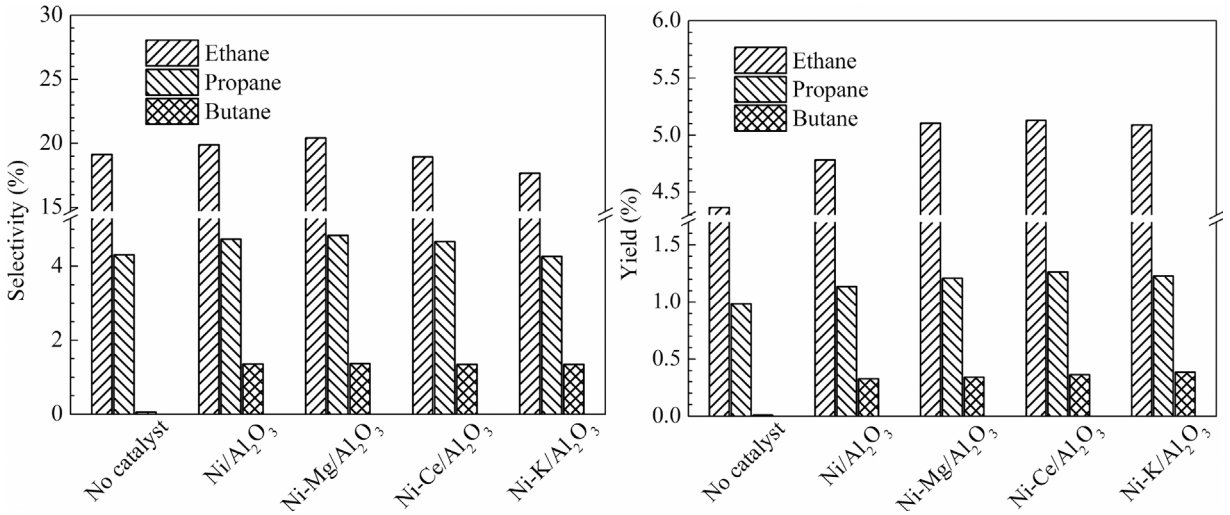

Fig. 7. Effect of different catalysts on (a) Selectivity and (b) Yield of C_2 − C_4 alkanes.

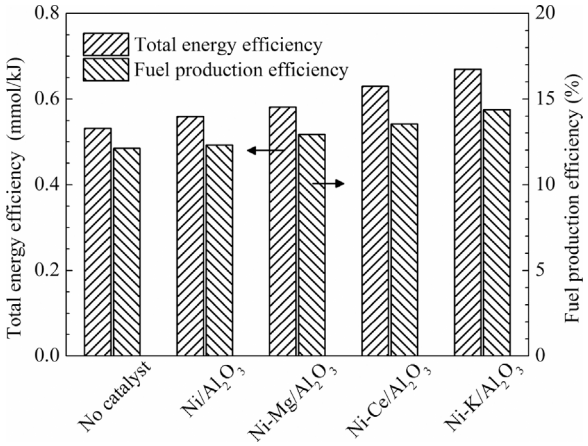

Fig. 8. Effect of different catalysts on the total energy efficiency and fuel production efficiency of the plasma reforming process.

comparing against the individual processes that using plasma-alone or catalysis-alone at the same temperature, as shown in Table 3. The significant synergy between the plasma and the Ni-based catalysts is highlighted by the conversion of CH_4, the yield of H_2 and propane, and the total energy efficiency of the reforming process. For instance, the yield of H_2 had a synergistic capacity of 9% in the absence of a promoter and reached a maximum of 31% using the NiKAl catalyst. The synergistic capacity of the plasma-catalytic process was significantly enhanced over the NiKAl catalyst compared to that using the NiAl catalyst. By contrast, the coupling of the plasma with the NiMgAl catalyst showed a negative synergistic capacity in CO_2 conversion and CO yield due to the obtained low CO_2 conversion in the plasma-catalytic reforming process.

Table 3
Effect of promoters on the synergistic capacity (SC) of the plasma-catalytic biogas reforming.

Catalyst	SC_C (%)		SC_Y (%)				SC_E (%)	SC_{FPE} (%)
	CH_4	CO_2	H_2	CO	C_2H_6	C_3H_8		
NiAl	8	7	9	−3	9	16	5	2
NiMgAl	24	−16	24	−1	17	23	9	7
NiCeAl	27	19	27	13	17	28	19	12
NiKAl	26	25	31	21	17	25	26	19

As shown in Figs. 5–8, the addition of K, Mg and Ce promoters showed a more pronounced effect on the reaction performance (conversion, selectivity, yield, and energy efficiency). The interaction between the DBD plasma and promoted Ni catalysts in the plasma reaction could be the main driving force contributed to the generation of the significant synergistic capacity in the plasma-catalytic biogas reforming [62–64].

3.3. Effect of promoters on carbon deposition

Three different forms of carbon deposition could be found on the catalyst surface according to the oxidation temperature of carbonaceous species in a TGA profile: active carbonaceous species (C_α), less active carbonaceous species (C_β) and inactive carbonaceous species (C_γ) [65,66]. In Fig. 9, the peak located at about 310 °C represented the active C_α species which usually exist as amorphous carbon and can be easily oxidized. The peak at about 520 °C showed the production of less active C_β species in the mixed form of amorphous and filamentous carbon [28,29,35]. A negligible amount of C_γ species (probably

Table 2
DBD plasma assisted dry reforming of methane.

Catalyst	Feed flow (ml min^{-1})	CH_4/CO_2	P (W)	Conversion (%)		Selectivity (%)		E (mmol kJ^{-1})	FPE (%)	Ref
				CH_4	CO_2	CO	H_2			
None	20	1:1	107	72.8	44.4	82.0	70.0	0.14	4.0	[60]
Ni/Al_2O_3	30	1:1	130	55.7	33.5	60.9	51.9	0.10	3.0	[61]
Ni/Al_2O_3	50	1:1	30	26.1	16.3	48.8	34.6	0.11	10.4	[19]
Ni/Al_2O_3	50	1:1	7.5	19.6	9.3	38.0	34.0	0.72	11.6	[13]
Ni/Al_2O_3	50	1:1	50	56.4	30.2	52.4	31.0	0.32	13.1	[15]
Ni/Al_2O_3	50	3:2	16	27.2	19.6	29.9	41.2	0.56	12.3	This work
$Ni-K/Al_2O_3$	50	3:2	16	31.6	22.8	31.3	43.3	0.67	14.4	This work

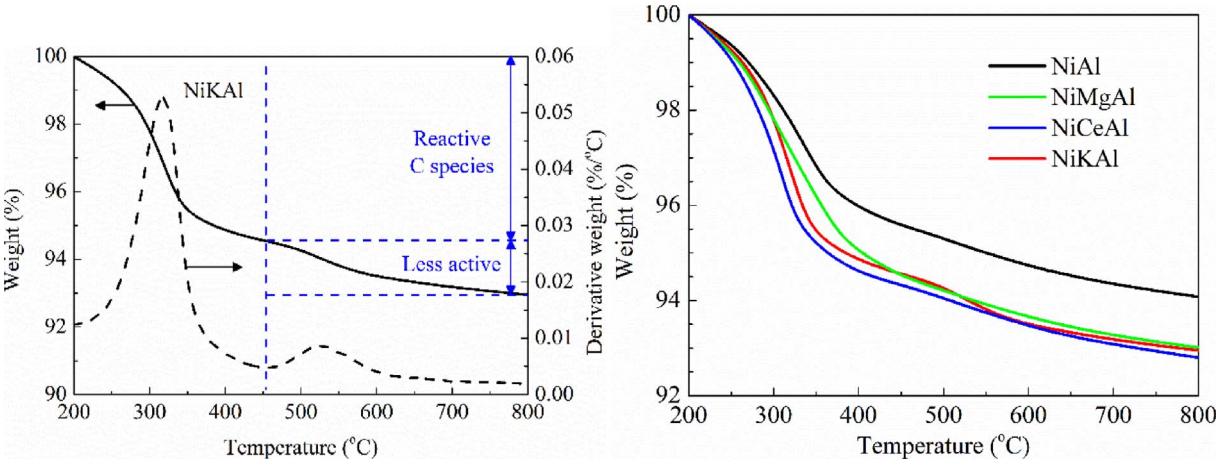

Fig. 9. (a) TGA profile of the spent NiKAl catalyst; (b) TGA profiles of the Ni catalysts after the plasma biogas reforming.

graphite) was observed on the spent catalysts.

Compared with the plasma reforming of biogas without a catalyst, the combination of plasma and the catalysts significantly enhanced the conversion of CH_4, while placing the K- and Ce-promoted catalysts in the plasma process also increased the conversion of CO_2. Compared with the NiAl catalyst, adding K, Ce and Mg promotors increased the carbon deposition on the catalyst surface, which can be clearly seen from the weight loss of these catalysts, as shown in Fig. 9 and Table 4. The amount of total carbon deposition followed the order of NiCeAl ≈ NiKAl ≈ NiMgAl > NiAl, in consistence with the CH_4 conversion (Fig. 6). This is plausible because the direct and indirect decomposition of CH_4 is an important source of carbon solid in plasma methane reforming reaction. In addition, the lowest amount of coke formation on the surface of the reacted NiAl catalyst could be related to the reduced acid sites on the catalyst (Fig. 4b) compared to the promoted catalysts as acid sites are responsible for the coke formation during reforming reactions [58].

In the plasma-catalytic biogas reforming, both the plasma gas phase reactions and plasma driven surface reactions could contribute to the formation of carbon deposition. In the gas phase reactions, the decomposition of CH_4 is initiated by electron impact dissociation of CH_4 to produce CH_x (x = 1–3) radicals (R1)–(R3) [13,15,16], followed by the recombination of radicals to form higher hydrocarbons or further decomposition via electron impact dissociation of CH_x (x = 1–3) radicals.

$$CH_4 + e^- \rightarrow CH_3 + H + e^- \quad (R1)$$

$$CH_4 + e^- \rightarrow CH_2 + H_2 + e^- \quad (R2)$$

$$CH_4 + e^- \rightarrow CH + H_2 + H + e^- \quad (R3)$$

In the presence of electrons with a high electron energy (> 14 eV), direct decomposition of methane or CH_x (x = 1–3) radicals by electrons could form solid carbon (R4)-(R7) in the gas phase or deposited onto the catalyst surfaces [15].

$$CH_4 + e^- \rightarrow C + 2H_2 + e^- \quad (R4)$$

Table 4
Ccarbon deposition on the spent catalysts.

Catalyst	Carbon deposition (wt.%)		
	Reactive	Less active	Total
NiAl	4.52	0.90	5.42
NiMgAl	5.59	0.95	6.54
NiCeAl	5.63	1.21	6.84
NiKAl	5.43	1.16	6.59

$$CH_3 + e^- \rightarrow C + H_2 + H + e^- \quad (R5)$$

$$CH_2 + e^- \rightarrow C + H_2 + e^- \quad (R6)$$

$$CH + e^- \rightarrow C + H + e^- \quad (R7)$$

On the surface of the catalyst, the adsorption and dissociation of CH_4 are important reaction pathways for the formation of solid carbon (R8)–(R11) [67].

$$CH_{4,ads} \rightarrow CH_{3,ads} + H_{ads} \quad (R8)$$

$$CH_{3,ads} \rightarrow CH_{2,ads} + H_{ads} \quad (R9)$$

$$CH_{2,ads} \rightarrow CH_{ads} + H_{ads} \quad (R10)$$

$$CH_{ads} \rightarrow C_{ads} + H_{ads} \quad (R11)$$

Where the subscript ads denotes adsorbed species.

However, the low temperature process inhibited the direct dissociation of CH_x (x = 1–4) to form carbon on the catalyst surface. The effect of the catalysts on the amount of carbon deposition also agree well with the NH_3-TPD results of the catalysts, as shown in Table 4 and Fig. 4. Compared to the NiAl catalyst, the addition of promoters increased the acidity of the catalysts, consequently enhancing the conversion of CH_4 and carbon deposition on the surface of the spent catalysts. However, previous studies reported that the addition of K, Mg and Ce promoters reduced carbon deposition on the catalyst surfaces in thermal catalytic biogas reforming compared to un-promoted catalysts, although the conversion of CH_4 was also dropped [28,29,31,35,37,38]. For instance, Sengupta et al. found that adding 5 wt.% MgO into a 15 wt.% Ni/Al_2O_3 catalyst significantly decreased carbon deposition on the spent catalyst from 24.5 wt.% to 14.4 wt.% after dry reforming of methane at 600 °C for 3 h [37]. Ozkara-Aydinoglu et al. reported that the carbon deposition on the spent Co/ZrO_2 catalyst was slightly decreased from 4% to 2.6% when using a Mg promoter [31]. In this work, although the use of the promoted catalysts increased the carbon deposition by 22%–26% compared to the NiAl catalyst, the increased carbon deposition was mainly in the form of reactive carbonaceous species (C_α), which contributed more than 80% of carbon deposited on the catalysts. C_α is reactive and can be easily oxidized by CO_2 or O species to form CO, consequently "regenerating" the catalysts. Interestingly, Debek et al. reported a similar phenomenon in thermal catalytic reforming of methane. They found that the addition of Ce promoter increased the amount of carbon deposition on the catalyst surface, but simultaneously decreased the oxidation temperature of the carbonaceous species [68]. In addition, even though the total amount of carbon deposition was increased by the addition of K promoter, only a negligible amount of C_γ species was found on the spent NiKAl catalyst

(Fig. 9(a)). This finding agrees well with the reported mechanism of K promoter suppressing the formation of graphite in the plasma reforming [48]. Most importantly, the carbon deposition on the surface of the promoted catalysts in this work (< 3.3 wt.% h^{-1}) was still less than the reported values (3.7–4.7 wt.% h^{-1}) obtained in thermal catalytic dry reforming of methane over promoted Ni/Al_2O_3 catalysts at high temperatures [29,37], even the CH_4/CO_2 molar ratio used in this work was much higher than that in previous works.

The stability of the promoted catalysts can also be confirmed by the stable conversion of CH_4 and CO_2 in the plasma-catalytic biogas reforming over the period (about 2 h) of the experiment. These findings indicate that the coupling of non-thermal plasma and promoted catalysts (except the NiMgAl catalyst) enhanced the conversion of CH_4 and CO_2, and the energy efficiency of the hybrid plasma process, but also increased the carbon deposition on the catalyst surface with reactive carbon species as the major one, which was still much less than that reported in thermal catalytic methane reforming at high temperatures. In addition, it is worth noting that catalysts that have shown poor activity in thermal catalytic reactions might work well in plasma-catalytic processes. Selecting appropriate catalysts with high selectivity, activity and stability is of primary importance for highly efficient plasma-catalytic chemical reactions.

4. Conclusions

Plasma-catalytic reforming of biogas over promoted Ni/Al_2O_3 catalysts has been carried out in a coaxial DBD reactor at 160 °C. Three different process modes: plasma-alone, catalysis-alone and plasma-catalysis were evaluated to get a better understanding of the plasma-catalytic coupling regime. Compared to the reforming reaction using either plasma-alone or catalysis-alone mode at the same temperature, the combination of the plasma with the Ni-based catalysts exhibited a low temperature synergistic effect at 160 °C, with enhanced CH_4 conversion, H_2 yield and energy efficiency of the hybrid plasma process. Compared to the NiAl catalyst, the use of the promoted catalysts in the plasma reforming process enhanced the conversion of CH_4, which can be associated with the enhanced acidity of the promoted catalysts. This finding also suggests that the acid sites on the surface of the catalysts contribute to the activation of CH_4 in the plasma-catalytic biogas reforming process. Note that in thermal catalytic biogas reforming, the use of these promotors reduced the conversion of CH_4. Interestingly, the effect of the promotors (K, Ce and Mg) on the reforming of biogas showed a different behaviour in the low temperature plasma process from the high temperature catalytic process in terms of the conversion of CH_4 and carbon deposition, which might be related to the temperature-dependent behaviour of the promotors. In the plasma-catalytic biogas reforming, the $Ni\text{-}K/Al_2O_3$ catalyst showed the best performance, enhancing the conversion of both CO_2 and CH_4, the yield of H_2, CO and C_2–C_4 alkanes and the energy efficiency of the plasma process; while the use of the Mg-promoted catalyst remarkably increased the H_2/CO molar ratio in the product due to the decreased CO_2 conversion, which could be associated to the weak CO_2 affinity on the catalyst surface. In addition, compared to the un-promoted NiAl catalyst, the use of the promoted catalysts increased the carbon deposition on the surface of the spent catalysts. However, the total amount of deposited carbon was still less than that reported in high temperature catalytic reforming processes. The TGA analysis of the spent catalysts showed that the increased carbonaceous species were mainly in the form of reactive carbon species, which can be easily oxidized by CO_2 and O and maintain the stability of the catalysts during the reforming reaction. These results also suggest those catalysts that have shown poor catalytic activity (e.g. conversion) in thermal catalytic reactions might work well in low temperature plasma-catalytic processes, and vice versa. The knowledge of selecting efficient and appropriate catalysts for plasma-catalytic chemical reactions to generate a synergistic effect is still very limited and more works are expected to breakdown traditional discipline boundaries and bridge the gaps between thermal catalysis and plasma catalysis.

Acknowledgement

The support of this work by the UK EPSRC SUPERGEN Hydrogen & Fuel Cell (H2FC) Programme (EP/J016454/1) ECR Project (Ref. EACPR_PS5768) and the Royal Society – Newton Advanced Fellowship (Ref. NA140303) is gratefully acknowledged. Y. X. Zeng acknowledges the PhD fellowship co-funded by the Doctoral Training Programme (DTP) at the University of Liverpool and Chinese Scholarship Council (CSC).

References

[1] N. Abatzoglou, S. Boivin, A review of biogas purification processes, Biofuels Bioprod. Biorefin. 3 (2009) 42–71.
[2] C. Perego, R. Bortolo, R. Zennaro, Gas to liquids technologies for natural gas reserves valorization: the eni experience, Catal. Today 142 (2009) 9–16.
[3] J.A. Velasco, L. Lopez, M. Velásquez, M. Boutonnet, S. Cabrera, S. Järås, Gas to liquids: a technology for natural gas industrialization in Bolivia, J. Nat. Gas Sci. Eng. 2 (2010) 222–228.
[4] H. Arbag, S. Yasyerli, N. Yasyerli, G. Dogu, T. Dogu, Enhancement of catalytic performance of Ni based mesoporous alumina by Co incorporation in conversion of biogas to synthesis gas, Appl. Catal. B: Environ. 198 (2016) 254–265.
[5] N. Charisiou, G. Siakavelas, K. Papageridis, A. Baklavaridis, L. Tzounis, D. Avraam, M. Goula, Syngas production via the biogas dry reforming reaction over nickel supported on modified with CeO_2 and/or La_2O_3 alumina catalysts, J. Nat. Gas Sci. Eng. 31 (2016) 164–183.
[6] S.D. Angeli, L. Turchetti, G. Monteleone, A.A. Lemonidou, Catalyst development for steam reforming of methane and model biogas at low temperature, Appl. Catal. B: Environ. 181 (2016) 34–46.
[7] H. Habibi, Mesoporous $MgO{\cdot}Al_2O_3$ nanopowder-supported meso–macroporous nickel catalysts: a new path to high-performance biogas reforming for syngas, RSC Adv. 6 (2016) 29576–29585.
[8] R. Dębek, M.E. Galvez, F. Launay, M. Motak, T. Grzybek, P. Da Costa, Low temperature dry methane reforming over Ce, Zr and CeZr promoted Ni–Mg–Al hydrotalcite-derived catalysts, Int. J. Hydrogen Energy 41 (2016) 11616–11623.
[9] R. Dębek, M. Motak, T. Grzybek, M. Galvez, P. Da Costa, A short review on the catalytic activity of hydrotalcite-derived materials for dry reforming of methane, Catalysts 7 (2017) 32.
[10] X. Tu, J.C. Whitehead, Plasma dry reforming of methane in an atmospheric pressure AC gliding arc discharge: co-generation of syngas and carbon nanomaterials, Int. J. Hydrogen Energy 39 (2014) 9658–9669.
[11] R. Snoeckx, R. Aerts, X. Tu, A. Bogaerts, Plasma-based dry reforming: a computational study ranging from the nanoseconds to seconds timescale, J. Phys. Chem. C 117 (2013) 4957–4970.
[12] J. Sentek, K. Krawczyk, M. Młotek, M. Kalczewska, T. Kroker, T. Kolb, A. Schenk, K.H. Gericke, K. Schmidt Szałowski, Plasma-catalytic methane conversion with carbon dioxide in dielectric barrier discharges, Appl. Catal. B: Environ. 94 (2010) 19–26.
[13] Y. Zeng, X. Zhu, D. Mei, B. Ashford, X. Tu, Plasma-catalytic dry reforming of methane over γ-Al_2O_3 supported metal catalysts, Catal. Today 256 (2015) 80–87.
[14] L. Wang, Y. Yi, C. Wu, H. Guo, X. Tu, One-step reforming of CO_2 and CH_4 into high-value liquid chemicals and fuels at room temperature by plasma-driven catalysis, Angew. Chem. Int. Ed. (2017), http://dx.doi.org/10.1002/anie.201707131.
[15] X. Tu, J.C. Whitehead, Plasma-catalytic dry reforming of methane in an atmospheric dielectric barrier discharge: understanding the synergistic effect at low temperature, Appl. Catal. B: Environ. 125 (2012) 439–448.
[16] W.-C. Chung, M.-B. Chang, Review of catalysis and plasma performance on dry reforming of CH_4 and possible synergistic effects, Renew. Sustain. Energy Rev. 62 (2016) 13–31.
[17] X. Tu, H.J. Gallon, M.V. Twigg, P.A. Gorry, J.C. Whitehead, Dry reforming of methane over a Ni/Al_2O_3 catalyst in a coaxial dielectric barrier discharge reactor, J. Phys. D: Appl. Phys. 44 (2011) 274007.
[18] Y. Zeng, X. Tu, Plasma-catalytic hydrogenation of CO_2 for the cogeneration of CO and CH_4 in a dielectric barrier discharge reactor: effect of argon addition, J. Phys. D: Appl. Phys. 50 (2017) 184004.
[19] D. Mei, B. Ashford, Y.-L. He, X. Tu, Plasma-catalytic reforming of biogas over supported Ni catalysts in a dielectric barrier discharge reactor: effect of catalyst supports, Plasma Process. Polym. 14 (2017) e1600076.
[20] K. Li, J.-L. Liu, X.-S. Li, X. Zhu, A.-M. Zhu, Warm plasma catalytic reforming of biogas in a heat-insulated reactor: dramatic energy efficiency and catalyst autoreduction, Chem. Eng. J. 288 (2016) 671–679.
[21] J.-L. Liu, H.-W. Park, W.-J. Chung, W.-S. Ahn, D.-W. Park, Simulated biogas oxidative reforming in AC-pulsed gliding arc discharge, Chem. Eng. J. 285 (2016) 243–251.
[22] X. Zhu, K. Li, J.-L. Liu, X.-S. Li, A.-M. Zhu, Effect of CO_2/CH_4 ratio on biogas reforming with added O_2 through an unique spark-shade plasma, Int. J. Hydrogen Energy 39 (2014) 13902–13908.
[23] N. Rueangjitt, C. Akarawitoo, S. Chavadej, Production of hydrogen-rich syngas from

biogas reforming with partial oxidation using a multi-stage AC gliding arc system, Plasma Chem. Plasma Process. 32 (2012) 583–596.
[24] Y.N. Chun, Y.C. Yang, K. Yoshikawa, Hydrogen generation from biogas reforming using a gliding arc plasma-catalyst reformer, Catal. Today 148 (2009) 283–289.
[25] X. Tao, F. Qi, Y. Yin, X. Dai, CO_2 reforming of CH_4 by combination of thermal plasma and catalyst, Int. J. Hydrogen Energy 33 (2008) 1262–1265.
[26] X. Tao, M. Bai, X. Li, H. Long, S. Shang, Y. Yin, X. Dai, CH_4–CO_2 reforming by plasma –challenges and opportunities, Prog. Energy Combust. Sci. 37 (2011) 113–124.
[27] D.H. Mei, S.Y. Liu, X. Tu, CO_2 reforming with methane for syngas production using a dielectric barrier discharge plasma coupled with Ni/Al_2O_3 catalysts: process optimization through response surface methodology, J. CO_2 Util. 21 (2017) 314–326.
[28] A. Nandini, K.K. Pant, S.C. Dhingra, K-, CeO_2-, and Mn-promoted Ni/Al_2O_3 catalysts for stable CO_2 reforming of methane, Appl. Catal. A: Gen. 290 (2005) 166–174.
[29] J. Juan-Juan, M.C. Román-Martínez, M.J. Illán-Gómez, Effect of potassium content in the activity of K-promoted Ni/Al_2O_3 catalysts for the dry reforming of methane, Appl. Catal. A: Gen. 301 (2006) 9–15.
[30] M.S. Fan, A.Z. Abdullah, S. Bhatia, Utilization of greenhouse gases through carbon dioxide reforming of methane over Ni–Co/MgO–ZrO_2: preparation, characterization and activity studies, Appl. Catal. B: Environ. 100 (2010) 365–377.
[31] Ş. Özkara-Aydınoğlu, A.E. Aksoylu, Carbon dioxide reforming of methane over Co-X/ZrO_2 catalysts (X = La, Ce, Mn, Mg, K), Catal. Commun. 11 (2010) 1165–1170.
[32] C.J. Liu, J.Y. Ye, J.J. Jiang, Y.X. Pan, Progresses in the preparation of coke resistant Ni-based catalyst for steam and CO_2 reforming of methane, ChemCatChem 3 (2011) 529–541.
[33] L. Xu, H. Song, L. Chou, Carbon dioxide reforming of methane over ordered mesoporous NiO–MgO–Al_2O_3 composite oxides, Appl. Catal. B: Environ. 108 (2011) 177–190.
[34] N. Wang, K. Shen, L. Huang, X. Yu, W. Qian, W. Chu, Facile route for synthesizing ordered mesoporous Ni–Ce–Al oxide materials and their catalytic performance for methane dry reforming to hydrogen and syngas, ACS Catal. 3 (2013) 1638–1651.
[35] Z. Alipour, M. Rezaei, F. Meshkani, Effect of alkaline earth promoters (MgO, CaO, and BaO) on the activity and coke formation of Ni catalysts supported on nano-crystalline Al_2O_3 in dry reforming of methane, J. Ind. Eng. Chem. 20 (2014) 2858–2863.
[36] R. Dębek, M. Radlik, M. Motak, M.E. Galvez, W. Turek, P. Da Costa, T. Grzybek, Ni-containing Ce-promoted hydrotalcite derived materials as catalysts for methane reforming with carbon dioxide at low temperature – on the effect of basicity, Catal. Today 257 (2015) 59–65.
[37] S. Sengupta, G. Deo, Modifying alumina with CaO or MgO in supported Ni and Ni–Co catalysts and its effect on dry reforming of CH_4, J. CO_2 Util. 10 (2015) 67–77.
[38] A.D. Ballarini, S.R. de Miguel, E.L. Jablonski, O.A. Scelza, A.A. Castro, Reforming of CH_4 with CO_2 on Pt-supported catalysts, Catal. Today 107–108 (2005) 481–486.
[39] L. Wang, Y.H. Yi, Y. Zhao, R. Zhang, J.L. Zhang, H.C. Guo, NH_3 decomposition for H_2 generation: effects of cheap metals and supports on plasma–catalyst synergy, ACS Catal. 5 (2015) 4167–4174.
[40] X. Zhu, X. Gao, X. Yu, C. Zheng, X. Tu, Catalyst screening for acetone removal in a single-stage plasma-catalysis system, Catal. Today 256 (2015) 108–114.
[41] K.J. Jeon, H.R. Moon, A.M. Ruminski, B. Jiang, C. Kisielowski, R. Bardhan, J.J. Urban, Air-stable magnesium nanocomposites provide rapid and high-capacity hydrogen storage without using heavy-metal catalysts, Nat. Mater. 10 (2011) 286–290.
[42] M.E. Gálvez, S. Ascaso, P. Stelmachowski, P. Legutko, A. Kotarba, R. Moliner, M.J. Lázaro, Influence of the surface potassium species in Fe–K/Al_2O_3 catalysts on the soot oxidation activity in the presence of NOx, Appl. Catal. B: Environ. 152–153 (2014) 88–98.
[43] G. Avgouropoulos, T. Ioannides, H. Matralis, Influence of the preparation method on the performance of CuO–CeO_2 catalysts for the selective oxidation of CO, Appl. Catal. B: Environ. 56 (2005) 87–93.
[44] X. Tu, H.J. Gallon, J.C. Whitehead, Plasma-assisted reduction of a NiO/Al_2O_3 catalyst in atmospheric pressure H_2/Ar dielectric barrier discharge, Catal. Today 211 (2013) 120–125.
[45] L. Ji, S. Tang, H. Zeng, J. Lin, K. Tan, CO_2 reforming of methane to synthesis gas over sol–gel-made Co/γ-Al_2O_3 catalysts from organometallic precursors, Appl. Catal. A: Gen. 207 (2001) 247–255.
[46] S. Tauster, S. Fung, R.L. Garten, Strong metal-support interactions. Group 8 noble metals supported on titanium dioxide, J. Am. Chem. Soc. 100 (1978) 170–175.
[47] A. Erdőhelyi, J. Cserényi, F. Solymosi, Activation of CH_4 and its reaction with CO_2 over supported Rh catalysts, J. Catal. 141 (1993) 287–299.
[48] D. San José-Alonso, M. Illán-Gómez, M. Román-Martínez, K and Sr promoted Co alumina supported catalysts for the CO_2 reforming of methane, Catal. Today 176 (2011) 187–190.
[49] X. Zhu, P. Huo, Y.P. Zhang, D.G. Cheng, C.J. Liu, Structure and reactivity of plasma treated Ni/Al_2O_3 catalyst for CO_2 reforming of methane, Appl. Catal. B: Environ. 81 (2008) 132–140.
[50] G. Wen, Y. Xu, Z. Xu, Z. Tian, Characterization and catalytic properties of the Ni/Al_2O_3 catalysts for aqueous-phase reforming of glucose, Catal. Lett. 129 (2009) 250–257.
[51] A.D. Mazzoni, M.A. Sainz, A. Caballero, E.F. Aglietti, Formation and sintering of spinels ($MgAl_2O_4$) in reducing atmospheres, Mater. Chem. Phys. (2002) 30–37.
[52] S. Damyanova, B. Pawelec, K. Arishtirova, J.L.G. Fierro, Ni-based catalysts for reforming of methane with CO_2, Int. J. Hydrogen Energy 37 (2012) 15966–15975.
[53] H.J. Gallon, X. Tu, J.C. Whitehead, Effects of reactor packing materials on H_2 production by CO_2 reforming of CH_4 in a dielectric barrier discharge, Plasma Process. Polym. 9 (2012) 90–97.
[54] D. Mei, X. Zhu, Y.-L. He, J.D. Yan, X. Tu, Plasma-assisted conversion of CO_2 in a dielectric barrier discharge reactor: understanding the effect of packing materials, Plasma Sources Sci. Technol. 24 (2015) 015011.
[55] M.C. Abello, A.P. Velasco, O.F. Gorriz, J.B. Rivarola, Temperature-programmed desorption study of the acidic properties of γ-alumina, Appl. Catal. A: Gen. 129 (1995) 93–100.
[56] M.A. Adnan, O. Muraza, S.A. Razzak, M.M. Hossain, H.I.d. Lasa, Iron oxide over silica-doped alumina catalyst for catalytic steam reforming of toluene as a surrogate tar biomass species, Energy Fuels 31 (2017) 7471–7481.
[57] J. Abbot, Role of Bronsted and Lewis acid sites during cracking reactions of alkanes, Appl. Catal. 47 (1989) 33–44.
[58] J. Ni, L.W. Chen, J.Y. Lin, S. Kawi, Carbon deposition on borated alumina supported nano-sized Ni catalysts for dry reforming of CH_4, Nano Energy 1 (2012) 674–686.
[59] N. Wang, Z. Xu, J. Deng, K. Shen, X. Yu, W. Qian, W. Chu, F. Wei, One-pot synthesis of ordered mesoporous NiCeAl oxide catalysts and a study of their performance in methane dry reforming, ChemCatChem 6 (2014) 1470–1480.
[60] Q. Wang, B.-H. Yan, Y. Jin, Y. Cheng, Investigation of dry reforming of methane in a dielectric barrier discharge reactor, Plasma Chem. Plasma Process. 29 (2009) 217–228.
[61] H.K. Song, J.-W. Choi, S.H. Yue, H. Lee, B.-K. Na, Synthesis gas production via dielectric barrier discharge over Ni/γ-Al_2O_3 catalyst, Catal. Today 89 (2004) 27–33.
[62] E.C. Neyts, Plasma-surface interactions in plasma catalysis, Plasma Chem. Plasma Process. 36 (2015) 185–212.
[63] E.C. Neyts, A. Bogaerts, Understanding plasma catalysis through modelling and simulation—a review, J. Phys. D: Appl. Phys. 47 (2014) 224010.
[64] M. Ramakers, I. Michielsen, R. Aerts, V. Meynen, A. Bogaerts, Effect of Argon or Helium on the CO_2 conversion in a dielectric barrier discharge, Plasma Process. Polym. 12 (2015) 755–763.
[65] Z. Zhang, X. Verykios, Carbon dioxide reforming of methane to synthesis gas over supported Ni catalysts, Catal. Today 21 (1994) 589–595.
[66] L. Zhang, L. Li, Y. Zhang, Y. Zhao, J. Li, Nickel catalysts supported on MgO with different specific surface area for carbon dioxide reforming of methane, J. Energy Chem. 23 (2014) 66–72.
[67] P.A. Nandini, K.K. Pant, S.C. Dhingra, R. Bhalla, Characterization and activity of K, CeO_2, and Mn promoted Ni/Al_2O_3 catalysts for carbon dioxide reforming of methane, Ind. Eng. Chem. Res. (2006) 7435–7443.
[68] R. Dębek, M. Motak, M.E. Galvez, P. Da Costa, T. Grzybek, Catalytic activity of hydrotalcite-derived catalysts in the dry reforming of methane: on the effect of Ce promotion and feed gas composition, React. Kinet. Mech. Catal. 121 (2017) 185–208.